

The pion beta and radiative electronic decays

D. Počanić^{1*}, for the PiBeta Collaboration

1 University of Virginia, Charlottesville, VA 22904-4714, USA

* pocanic@virginia.edu

11 May 2021



Review of Particle Physics at PSI
doi:10.21468/SciPostPhysProc.2

Abstract

As the lightest meson, pion offers unique opportunities for measuring parameters and testing limits of the Standard Model (SM). The PiBeta experiment, carried out at PSI, focused on SM tests accessible through the pion beta, $\pi^+ \rightarrow \pi^0 e^+ \nu_e(\gamma)$, and electronic radiative, $\pi^+ \rightarrow e^+ \nu_e \gamma$, decay channels. We review the PiBeta experiment, and update the pion beta decay branching ratio $B_{\pi\beta}^{\text{exp}} = 1.038(6)_{\text{tot}} \times 10^{-8}$, along with the corresponding derived value of the Cabibbo-Kobayashi-Maskawa matrix element $V_{ud} = 0.9738(28)$.

24.1 Motivation

The unitary Cabibbo-Kobayashi-Maskawa (CKM) quark mixing matrix embodies some of the central parameters of the three-generation Standard Model. Departure from CKM matrix unitarity would signal the existence of “beyond Standard Model” (BSM) physics, i.e., processes and particles not included in the SM. The most sensitive test of the CKM matrix unitarity is via $|V_u|^2$, the squared norm of the first row, which, given the smallness of $|V_{ub}|^2 \simeq 10^{-5}$, simplifies as:

$$|V_u|^2 \equiv |V_{ud}|^2 + |V_{us}|^2 + |V_{ub}|^2 \simeq |V_{ud}|^2 + |V_{us}|^2, \quad \text{with} \quad |V_u|^2 = 1 + \Delta_{\text{CKM}}. \quad (24.1)$$

Since $|V_{ud}|^2 \approx 0.95$ dominates $|V_u|^2$, the uncertainty ΔV_{ud} is critically important in evaluating Δ_{CKM} . In spite of notable improvements in measurement and theoretical precision since the 1980s, a shortfall of $\Delta_{\text{CKM}} \sim -3\sigma$ has persisted for much of the past three decades. The discovery potential inherent in precision tests of CKM unitarity has motivated a worldwide effort. A summary of the present status of CKM unitarity tests is given in [1]. The most precise evaluations of V_{ud} have relied on the $0^+ \rightarrow 0^+$ superallowed Fermi (SAF) nuclear beta decays (for the most recent compilation see [2]). Despite the impressive experimental precision achieved in determining SAF $f t$ values, uncertainties related to the complex structure of participating nuclei remain, motivating the quest for V_{ud} evaluation in beta decays of simpler systems: neutrons and pions. Of the two, the pion beta semileptonic decay $\pi^+ \rightarrow \pi^0 e^+ \nu_e(\gamma)^1$, or $\pi_{e3(\gamma)}$, is the theoretically cleanest [3]. Given the small accessible phase space, π_{e3} decay is very rare: $B_{\pi\beta} \simeq 10^{-8}$. Neutron beta decay is not suppressed, but requires two measurements for an independent determination of V_{ud} : the lifetime, τ_n , and the axial-vector coupling, $g_A = G_A/G_V$, (for further details and current status see [1, 4–6]).

The international PiBeta collaboration [7], led by the University of Virginia group, was formed in the 1990s with the goal of measuring the pion beta decay branching ratio to a

¹A γ in parentheses denotes an undetected, usually soft photon. For brevity, in further text the (γ) will be dropped and implied; a detected photon in radiative processes will be explicitly denoted with a γ .

37 precision of 0.5% at the Paul Scherrer Institute. Achieving this goal also requires accurate
 38 identification and detection of background and normalization decays: pion radiative electronic
 39 $\pi^+ \rightarrow e^+ \nu_e \gamma$, or $\pi_{e2\gamma}$, pion electronic $\pi^+ \rightarrow e^+ \nu_e$, or π_{e2} , radiative muon $\mu^+ \rightarrow e^+ \nu_e \bar{\nu}_\mu \gamma$, and
 40 ordinary muon $\mu^+ \rightarrow e^+ \nu_e \bar{\nu}_\mu$ decay. Each of these processes illuminates interesting aspects of
 41 SM/BSM physics. Muon decays will not be discussed here, while the electronic, π_{e2} decay is
 42 discussed in more detail in [8].

43 Unlike its muonic equivalent $\pi_{\mu2\gamma}$, the radiative electronic decay, $\pi_{e2\gamma}$, is not completely
 44 dominated by purely electromagnetic (QED) “inner” bremsstrahlung (IB). It also receives
 45 strong “structure-dependent” (SD) QCD contributions, parameterized in terms of F_V and F_A ,
 46 the vector and the axial-vector form factors, respectively. Direct determination of $F_{A,V}$ is
 47 possible through a precise measurement of the differential branching ratio, or decay rate
 48 $d^2\Gamma_{\pi_{e2\gamma}}/dE_e dE_\gamma$, over a suitably large portion of the decay phase space [9, 10]. Precise val-
 49 ues of F_A and F_V provide information on nonperturbative QCD, such as the pion polarizabil-
 50 ities, and generally enter certain low energy (chiral) constants, LECs (for more details see,
 51 e.g., [11, 12]). On the other hand, a kinematically broad sample of $\pi_{e2\gamma}$ decays makes it pos-
 52 sible to set limits on values of form factors other than $F_{A,V}$, that, if nonzero, would indicate
 53 presence of BSM particles or processes. PiBeta has pursued both of these research paths, as
 54 discussed below.

55 24.2 The PiBeta apparatus

56 The PiBeta apparatus, schematically shown in Figure 24.1, detected π^+ decays at rest in a
 57 solid cylindrical active target (AT), placed at the center of a pure CsI, 240-element spheri-
 58 cal electromagnetic shower calorimeter. Prior to stopping, pions passed through a pair of
 59 scintillation detectors (BC and AD) separated by a ~ 3.5 m flight path. The segmented target
 60 was surrounded by two MWPC tracking detectors, and a fast 20-element hodoscope, shown
 61 schematically in Figure 24.2. The apparatus acquired data during a “ π -stop” gate spanning
 62 $t \simeq -50$ to 200 ns relative to a pion stop time ($t = 0$) in the target, with a break of ~ 10 ns at

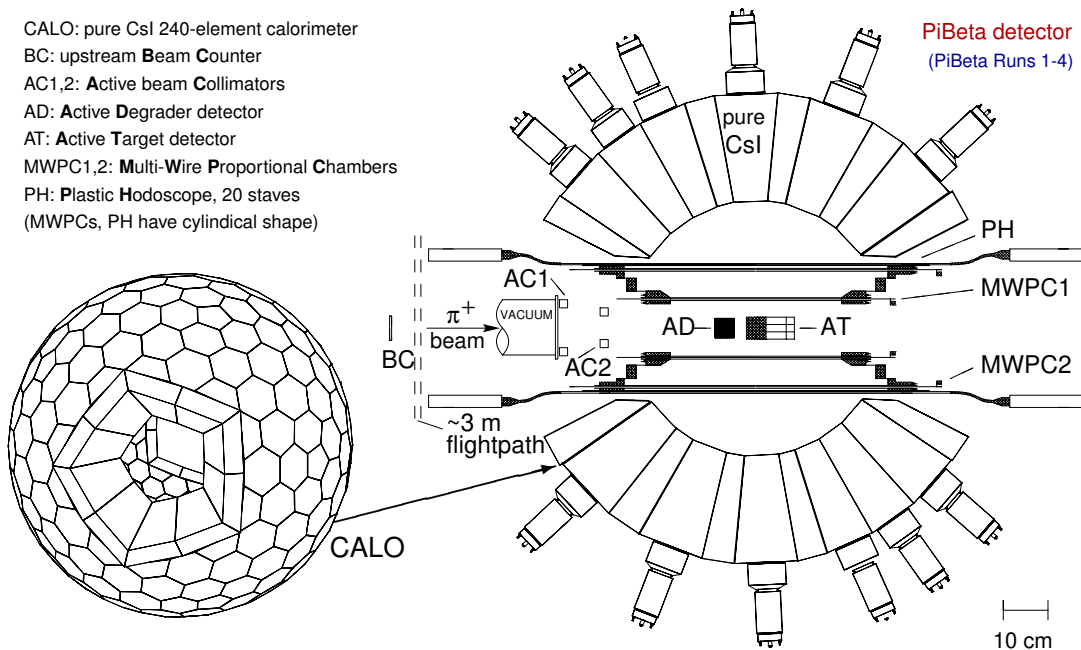


Figure 24.1: Schematic cross section of the PiBeta apparatus, with its main components labeled. For details concerning the detector performance see [13].

24.3 The pion beta decay: $\pi^+ \rightarrow \pi^0 e^+ \nu_e(\gamma)$

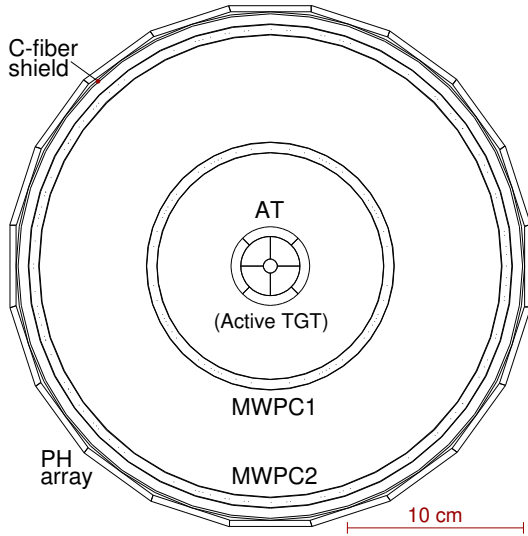


Figure 24.2: Axial (beam) view of the central detector region used in PiBeta Runs 1–3, and first half of Run 4. Outward from center: (i) the 9-element segmented active target AT, (ii) cylindrical MWPC1 and MWPC2 trackers, (iii) thin cylindrical carbon-fiber shield around MWPC2, and (iv) the 20-element plastic hodoscope (PH) array with approximate outer diameter of $\text{\O}30$ cm. Pion stopping rates in the inner five (fiducial) target elements were roughly matched; AT outer ring elements served for decay particle tracking. The BC, AD, AT and PH detectors were made of fast plastic scintillator.

63 $t = 0$ because of high rates of hadronic reactions by beam pions in AD and AT. The calorimeter
 64 meter modules were sized such that, on average, a crystal impacted centrally by a 70 MeV e^+ or
 65 γ would contain over 90% of the resulting shower energy. The location and energy of each
 66 distinct shower in an event were extracted for trigger purposes from continuous analog sig-
 67 nals of overlapping clusters of 7–9 modules. A dozen trigger configurations, combining
 68 calorimeter and beam detector hit patterns of interest, were used to acquire the studied and
 69 normalization decay events, as well as all relevant background processes. Further details of
 70 the design and performance of the apparatus are given in [13]. For a discussion of the PiBeta
 71 technique in a broader context, see [14].

72 24.3 The pion beta decay: $\pi^+ \rightarrow \pi^0 e^+ \nu_e(\gamma)$

73 PiBeta measurements were carried out in four run periods, using 114 MeV/c beam in the π E1
 74 beamline at PSI. Over 6.4×10^4 π_{e3} events were acquired in high-rate Runs 1-3 (1999-2001),
 75 with $\sim 10^6$ π_{stop}^+ /s in the target. Run 4 (2004), with $10^4 - 10^5$ π_{stop}^+ /s in the target, focused
 76 on the radiative decay $\pi_{e2\gamma}$. The π_{e3} decay signal, two energetic, nearly back to back neutral
 77 showers in the calorimeter, initiated by the two photons from $\pi^0 \rightarrow \gamma\gamma$ decay, is robust and re-
 78 quired minimal background subtractions. Figure 24.3 illustrates the quality of the PiBeta π_{e3}
 79 event sample. The $\theta_{\gamma_1\gamma_2}$ distribution, uniquely shaped by the decay kinematics and the shower

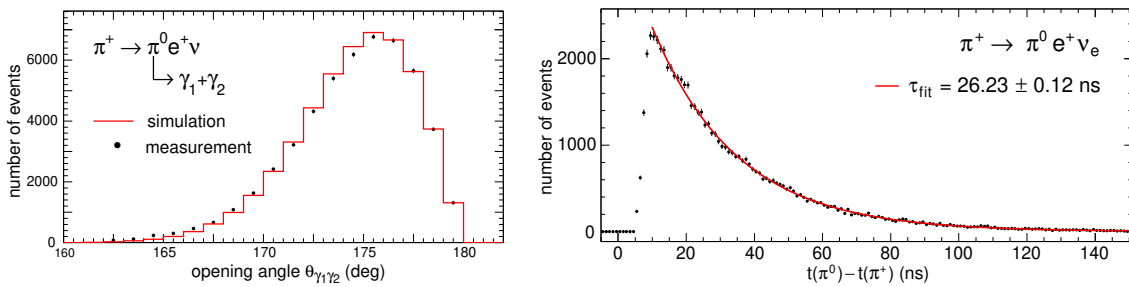


Figure 24.3: Left: measured photon-photon opening angle in $\pi^0 \rightarrow \gamma\gamma$, compared to a realistic Monte Carlo simulation. Right: decay time distribution for π_{e3} events. Events within ~ 10 ns of the π^+ stop in AT were not recorded due to high prompt hadronic background.

80 response of the calorimeter, is not reproduced in other processes. The decay time distribution
 81 is purely exponential, and agrees well with the known pion lifetime of 26.033(5) ns [1]. The
 82 $\pi^+ \rightarrow e^+ \nu_e(\gamma)$ electronic decay events were used for branching ratio normalization. While the
 83 two decays shared many of the same systematics, such as the spatial and temporal distributions
 84 of the parent pions, and very similar acceptances, the π_{e2} signal had a significant background
 85 from the ‘‘Michel’’ $\mu^+ \rightarrow e^+ \nu \bar{\nu}(\gamma)$ decays. Details of the analysis and results for the π_{e3} branch-
 86 ing ratio are discussed in [15]. Two values of $B_{\pi\beta} = \Gamma(\pi^+ \rightarrow \pi^0 e^+ \nu(\gamma))/\Gamma(\pi^+ \rightarrow \mu^+ \nu(\gamma))$
 87 were evaluated and reported: one normalized to the accepted 2004 experimental average of
 88 $R_{e/\mu}^{\pi\text{-exp}} = \Gamma(\pi \rightarrow e \bar{\nu}(\gamma))/\Gamma(\pi \rightarrow \mu \bar{\nu}(\gamma)) = 1.230(4) \times 10^{-4}$ (‘‘exp-norm’’), and the second to the
 89 established theoretical value $R_{e/\mu}^{\pi\text{-th}} = 1.2352(5) \times 10^{-4}$ (‘‘theo-norm’’):

$$B_{\pi\beta}^{\text{exp-norm}} = 1.036(4)_{\text{stat}}(4)_{\text{syst}}(3)_{\pi_{e2}} \times 10^{-8}, \quad (24.2)$$

$$B_{\pi\beta}^{\text{theo-norm}} = 1.040(4)_{\text{stat}}(4)_{\text{syst}} \times 10^{-8}, \quad (24.3)$$

90 where the statistical (stat), systematic (syst) and π_{e2} normalization uncertainties are separated
 91 out. Since 2004, the π_{e2} branching ratio has become better known, $R_{e/\mu}^{\pi\text{-exp}} = 1.2327(23) \times 10^{-4}$
 92 [1, 16]. This leads to an update of the PiBeta π_{e3} branching ratio result

$$B_{\pi\beta}^{\text{exp-norm}} = 1.038(4)_{\text{stat}}(4)_{\text{syst}}(2)_{\pi_{e2}} \times 10^{-8} = 1.038(6)_{\text{tot}} \times 10^{-8}. \quad (24.4)$$

93 We note that the extraordinary sensitivity of pion beta decay afforded by the SM, with relative
 94 uncertainty (excluding the free parameter V_{ud}) of $\sim 2 \times 10^{-4}$ dominated by the radiative cor-
 95 rections [17], cannot be tested experimentally at the current precision of $\Delta B_{\pi\beta}/B_{\pi\beta} \simeq 0.006$.
 96 The same observation applies to the derived value of V_{ud} , now updated to

$$V_{ud}^{\pi\beta} = 0.9738(28), \quad (24.5)$$

97 which, while in excellent agreement with the PDG average $V_{ud} = 0.97370(14)$ [1], is 20 times
 98 less precise.

99 24.4 Pion radiative electronic decay: $\pi^+ \rightarrow e^+ \nu_e \gamma$

100 In addition to the fundamental physics motivations introduced in Section 24.1 (weak pionic
 101 form factors, inputs to LECs, limits on BSM contributions), pion radiative electronic decay
 102 generates background events for the pion beta (π_{e3}) signal, in large enough numbers to re-
 103 quire a correction (the reverse also holds). For all these reasons, the PiBeta collaboration has
 104 extensively studied the $\pi_{e2\gamma}$ decay.

105 Prior to the early 2000s, data on the $\pi_{e2\gamma}$ decay were scarce, and contained significant
 106 ambiguities. The doubly differential decay rate $d^2\Gamma_{\pi_{e2\gamma}}/dE_e dE_\gamma$ is separated into structure
 107 dependent terms: $SD^+ \propto (F_A + F_V)^2$, $SD^- \propto (F_A - F_V)^2$, the purely-QED IB , and several
 108 interference terms of the linear amplitudes, of which the most important are S_{int}^+ and S_{int}^- , the
 109 $IB \cdot (F_A + F_V)$ and $IB \cdot (F_A - F_V)$ terms, respectively. For simplicity in the analysis, dimensionless
 110 energy variables are routinely used and are limited to unity: $x, y = 2E_{\gamma,e}/m_\pi \in (0, 1)$. Since
 111 $(F_A + F_V)^2/(F_A - F_V)^2 \simeq 8$, SD^+ is the dominant QCD term in the decay. Further, its study is
 112 made more accessible by the fact that SD^+ peaks for $y \in (0.9, 1)$, and large x , where the IB
 113 term nearly vanishes. SD^- , on the other hand, peaks near the diagonal, $x + y = 1$, where IB
 114 is greatest, and dwarfs SD^- by several orders of magnitude. Consequently, pre-2000 studies
 115 used the conserved vector current (CVC) theoretical value for F_V (derived from the π^0 meson
 116 lifetime), and reported the ratio $\gamma \equiv F_A/F_V$ extracted from measurements. Early measure-
 117 ments, along with the inconsistencies and hints of BSM phenomena through a nonzero value
 118 for F_T , the tensor form factor, are discussed in detail in [14].

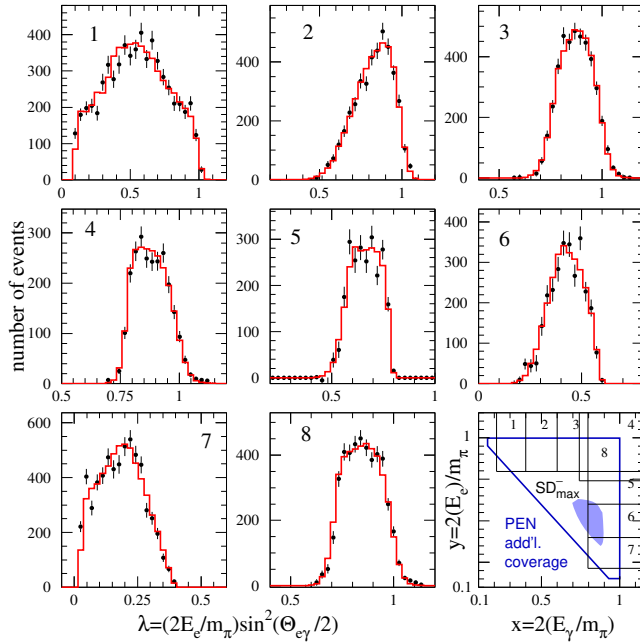


Figure 24.4: Measured (points) and simulated (histogram) values of $\pi_{e2\gamma}$ variable λ for eight (x, y) regions, mapped in the lower right panel. Triangle: added coverage by PEN [8]. Shaded contour: region of peak relative SD^- contribution.

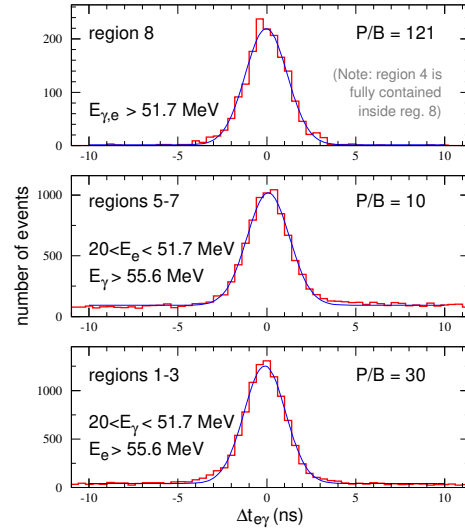


Figure 24.5: Plots of $\Delta t_{e\gamma}$, for three phase space regions in $\pi_{e2\gamma}$ decay, defined in Figure 24.4. Accidental background was low for all regions, reflected in the peak to background (P/B) values. Region 4/8 was dominated by Run 1–3 data; Run 4 data dominated the rest.

119 Against this backdrop, the PiBeta collaboration collected and analyzed over 4×10^4 $\pi_{e2\gamma}$
 120 events in Runs 1–3, and published the results in [13]. The precision in γ was improved by a
 121 factor of four over prior world average, but a significant deficit of events was observed in a
 122 region of high x and low y . The high beam rate, and trigger configuration during Runs 1–3,
 123 challenged the $\pi_{e2\gamma}$ decay systematics in this kinematic regime.

124 Given the above, in 2004 the PiBeta collaboration carried out Run 4 at much lower beam
 125 rate ($\sim 10^5 \pi_{\text{stop}}/\text{s}$), focused on low-threshold $\pi_{e2\gamma}$ events. This made possible a precise cali-
 126 bration of subtle calorimeter gain differences in the low- and high-threshold triggers, the key to
 127 resolving previously observed inconsistencies. Results of the combined Run 1–4 data set anal-
 128 ysis, with over 6.5×10^4 $\pi_{e2\gamma}$ events, were published in [18]. Kinematic coverage is shown
 129 in Figure 24.4, while Figure 24.5 illustrates the low level of accidental background present in
 130 the $e^+ - \gamma$ time difference data. Data in Figure 24.4 are presented in terms of $\lambda = y \sin^2(\theta_{e\gamma}/2)$,
 131 where $\theta_{e\gamma}$ is the reconstructed $e^+ - \gamma$ opening angle. (Unlike y , λ retains the constant 0–1 value
 132 range regardless of x .) Agreement with the simulation based on best-fit values for F_A and F_V
 133 is excellent in all regions.

134 Contours of the best-fit values for F_A and F_V are shown in Figure 24.6. The thin shape of
 135 the resulting ellipse reflects the $\sim 1\%$ precision of the measurement of $F_A + F_V$ (SD^+ term),
 136 and the much lower sensitivity to $F_A - F_V$, i.e., SD^- . The narrow linear dependence of F_A
 137 on F_V reported in [18] enables future updates of the best-fit value of F_A based on improved
 138 evaluations of F_V^{CVC} .

139 Figure 24.6 also plots a , the slope parameter of F_V with respect to the momentum transfer
 140 to the lepton pair $q_{e\nu}^2$, a first such result, made possible by the broad combined kinematic
 141 coverage of PiBeta Runs 1–4. The slope is in qualitative agreement with the χ PT calculation
 142 of Mateu and Portoles [19].

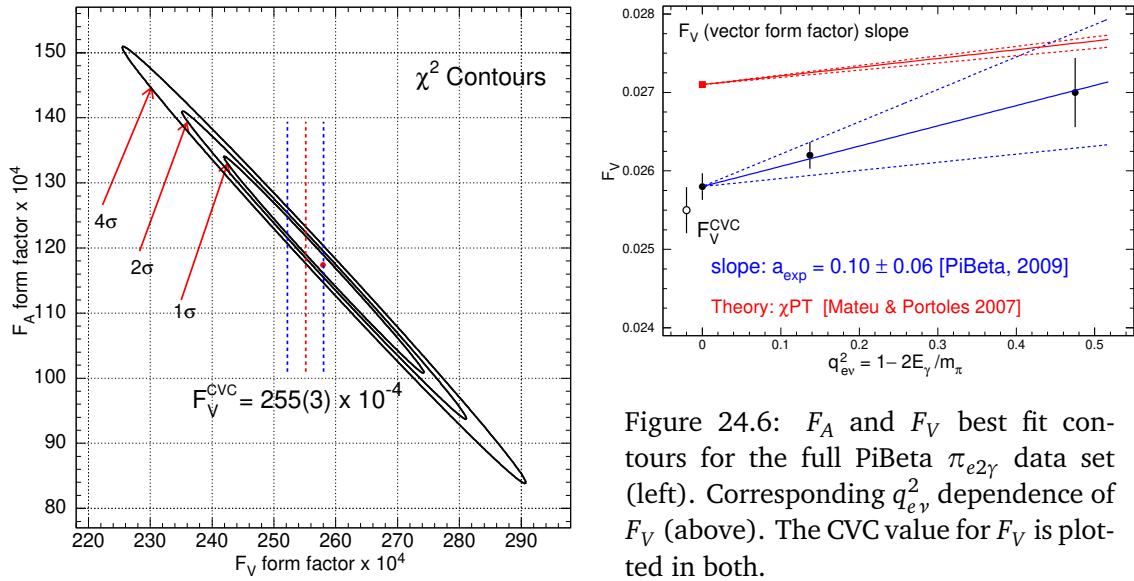


Figure 24.6: F_A and F_V best fit contours for the full PiBeta $\pi_{e2\gamma}$ data set (left). Corresponding $q_{e\gamma}^2$ dependence of F_V (above). The CVC value for F_V is plotted in both.

143 Analysis of the integral $\pi_{e2\gamma}$ decay rate yielded the primary result: branching ratio for the
 144 kinematic region $E_\gamma > 10$ MeV and $\theta_{e\gamma} > 40^\circ$ of $B^{\text{exp}} = 73.86(54) \times 10^{-8}$. At $< 1\%$, this result
 145 marked a ~ 20 -fold precision improvement over previous measurements [1]. The excellent fit
 146 of the $\pi_{e2\gamma}$ differential decay rates has led to the arguably most important result of this work,
 147 the limit on a possible admixture of the tensor interaction $-5.2 \times 10^{-4} < F_T < 4.0 \times 10^{-4}$ with
 148 90% confidence [18]. To date, this limit provides the strongest constraint on a possible BSM
 149 tensor coupling [20].

150 24.5 Conclusions and path forward

151 The PiBeta research program has produced an order of magnitude improvement in the pre-
 152 cision of the π_{e3} and $\pi_{e2\gamma}$ branching ratios, and related SM observables, low energy QCD
 153 parameters (LECs), and a leading limit on BSM tensor coupling.

154 PEN, the successor experiment to PiBeta, has focused on π_{e2} decay [8], and expanded the
 155 $\pi_{e2\gamma}$ kinematic coverage (Figure 24.4), fully enclosing the region of peak SD^- /total relative
 156 yield². This is a modest improvement. A new, dedicated experiment would be needed to
 157 achieve greater sensitivity.

158 The scientific case is mounting for a new generation of experiment to fully exploit the
 159 precision of the SM description of pion decays, and realize the potential to settle the decades-
 160 old question of CKM unitarity in a process free from complex nuclear structure corrections.

161 Acknowledgments

162 This work has been supported by the U.S. National Science Foundation, the Paul Scherrer
 163 Institute, and the Russian Foundation for Basic Research.

164 References

- 165 [1] P. Zyla *et al.*, *Review of Particle Physics*, PTEP **2020**(8), 083C01 (2020),
 166 doi:[10.1093/ptep/ptaa104](https://doi.org/10.1093/ptep/ptaa104).

²Even at its peak relative to other terms, SD^- locally contributes only $\sim 8\%$ of the decays.

- 167 [2] J. Hardy and I. Towner, *Superallowed $0^+ \rightarrow 0^+$ nuclear β decays: 2020 critical survey, with implications for V_{ud} ...*, Phys. Rev. C **102**(4), 045501 (2020),
168 doi:[10.1103/PhysRevC.102.045501](https://doi.org/10.1103/PhysRevC.102.045501).
169
- 170 [3] A. Czarnecki, W. Marciano and A. Sirlin, *Pion beta decay and Cabibbo-Kobayashi-Maskawa unitarity*, Phys. Rev. D **101**(9), 091301 (2020), doi:[10.1103/PhysRevD.101.091301](https://doi.org/10.1103/PhysRevD.101.091301),
171 [1911.04685](https://arxiv.org/abs/1911.04685).
172
- 173 [4] B. Märkisch *et al.*, *Measurement of the weak axial-vector coupling constant in the decay of free neutrons using ...*, Phys. Rev. Lett. **122**(24), 242501 (2019),
174 doi:[10.1103/PhysRevLett.122.242501](https://doi.org/10.1103/PhysRevLett.122.242501), [1812.04666](https://arxiv.org/abs/1812.04666).
175
- 176 [5] A. Czarnecki, W. Marciano and A. Sirlin, *Neutron lifetime and axial coupling connection*,
177 Phys. Rev. Lett. **120**(20), 202002 (2018), doi:[10.1103/PhysRevLett.120.202002](https://doi.org/10.1103/PhysRevLett.120.202002), [1802.01804](https://arxiv.org/abs/1802.01804).
178
- 179 [6] S. Baeßler, J. Bowman, S. Penttilä and D. Počanić, *New precision measurements of free neutron beta decay with cold neutrons*, J. Phys. G **41**, 114003 (2014), doi:[10.1088/0954-3899/41/11/114003](https://doi.org/10.1088/0954-3899/41/11/114003), [1408.4737](https://arxiv.org/abs/1408.4737).
180
181
- 182 [7] *Pibeta experiment home page*, <http://pibeta.phys.virginia.edu>.
- 183 [8] D. Počanić, *Pion electronic decay and lepton universality*, this volume of SciPost Phys. Proc., paper 025 (2021).
184
- 185 [9] P. De Baenst and J. Pestieau, *Extension of Cabibbo's theory to radiative leptonic decays of pseudoscalar mesons*, Nuovo Cim. A **53**, 407 (1968), doi:[10.1007/BF02800120](https://doi.org/10.1007/BF02800120).
186
- 187 [10] D. Bryman, P. Depommier and C. Leroy, *$\pi \rightarrow e\nu$, $\pi \rightarrow e\nu\gamma$ decays and related processes*, Phys. Rept. **88**, 151 (1982), doi:[10.1016/0370-1573\(82\)90162-4](https://doi.org/10.1016/0370-1573(82)90162-4).
188
- 189 [11] J. Donoghue, E. Golowich and B. Holstein, *Dynamics of the standard model*, Cambridge University Press, Cambridge, doi:[10.1017/CBO9780511524370](https://doi.org/10.1017/CBO9780511524370) (1992).
190
- 191 [12] J. Bijnens and G. Ecker, *Mesonic low-energy constants*, Ann. Rev. Nucl. Part. Sci. **64**, 149 (2014), doi:[10.1146/annurev-nucl-102313-025528](https://doi.org/10.1146/annurev-nucl-102313-025528), [1405.6488](https://arxiv.org/abs/1405.6488).
192
- 193 [13] E. Frlež *et al.*, *Design, commissioning and performance of the PIBETA detector at PSI*, Nucl. Instrum. Meth. A **526**, 300 (2004), doi:[10.1016/j.nima.2004.03.137](https://doi.org/10.1016/j.nima.2004.03.137), [hep-ex/0312017](https://arxiv.org/abs/hep-ex/0312017).
194
- 195 [14] D. Počanić, E. Frlež and A. van der Schaaf, *Experimental study of rare charged pion decays*, J. Phys. G **41**, 114002 (2014), doi:[10.1088/0954-3899/41/11/114002](https://doi.org/10.1088/0954-3899/41/11/114002), [1407.2865](https://arxiv.org/abs/1407.2865).
196
- 197 [15] D. Počanić *et al.*, *Precise measurement of the $\pi^+ \rightarrow \pi^0 e^+ \nu$ branching ratio*, Phys. Rev. Lett. **93**, 181803 (2004), doi:[10.1103/PhysRevLett.93.181803](https://doi.org/10.1103/PhysRevLett.93.181803), [hep-ex/0312030](https://arxiv.org/abs/hep-ex/0312030).
198
- 199 [16] A. Aguilar-Arevalo *et al.*, *Improved measurement of the $\pi \rightarrow e\nu$ branching ratio*, Phys. Rev. Lett. **115**(7), 071801 (2015), doi:[10.1103/PhysRevLett.115.071801](https://doi.org/10.1103/PhysRevLett.115.071801), [1506.05845](https://arxiv.org/abs/1506.05845).
200
- 201 [17] A. Czarnecki, W. J. Marciano and A. Sirlin, *Radiative corrections to neutron and nuclear beta decays revisited*, Phys. Rev. D **100**(7), 073008 (2019),
202 doi:[10.1103/PhysRevD.100.073008](https://doi.org/10.1103/PhysRevD.100.073008), [1907.06737](https://arxiv.org/abs/1907.06737).
203
- 204 [18] M. Bychkov *et al.*, *New precise measurement of the pion weak form factors in $\pi^+ \rightarrow e^+ \nu\gamma$ decay*, Phys. Rev. Lett. **103**, 051802 (2009), doi:[10.1103/PhysRevLett.103.051802](https://doi.org/10.1103/PhysRevLett.103.051802),
205 [0804.1815](https://arxiv.org/abs/0804.1815).
206

- 207 [19] V. Mateu and J. Portoles, *Form-factors in radiative pion decay*, Eur. Phys. J. C **52**, 325
208 (2007), doi:[10.1140/epjc/s10052-007-0393-5](https://doi.org/10.1140/epjc/s10052-007-0393-5), [0706.1039](https://arxiv.org/abs/0706.1039).
- 209 [20] T. Bhattacharya *et al.*, *Probing novel scalar and tensor interactions from (ultra)cold neu-*
210 *trons to the LHC*, Phys. Rev. D **85**, 054512 (2012), doi:[10.1103/PhysRevD.85.054512](https://doi.org/10.1103/PhysRevD.85.054512),
211 [1110.6448](https://arxiv.org/abs/1110.6448).